JOURNAL OF OPTOELECTRONICS AND ADVANCED MATERIALS, Vol. 10, No. 12, December 2008, p. 3233 - 3236

Properties of iron modified mesophase pitch

C. BANCIU*, A. BARA, I. IOANA, A. M. BONDAR, R. MIREA, G. STOIAN, E. PATROI
National Institute for Research and Development in Electrical Engineering INCDIE ICPE-CA
313 Splaiul Unirii, 030138, Bucharest 3, Romania

The multifunctional composites were obtained by mixing carbon-coated nano iron and iron oxide with petroleum pitch. The additivated petroleum pitch was heat treated at mesophase condensation temperature (460°C). The structural and functional changes induced by different types of additives were analyzed.

(Received October 18, 2008; accepted November 27, 2008)

Keywords: Mesophase pitch, Carbon-coated nanoiron, Iron oxide, Composites

1. Introduction

The composites with a carbon phase containing dispersed metal nanoparticles have been extensively studied because they are widely used in electronic, electrical and magnetic devices, as adsorbents, antibacterial agents and oxidation/reduction catalysts [1]. There are lot of methods of inducing nanometric metal particles in a carbon matrix using different precursors with a further heat treatment, up to 1000°C as: (1) from a petroleum residue by heating at 420°C with ferrocene under pressure [2]; (2) from a furan resin or polyfurfuryl alcohol and ferrocene [3]; (3) or by a sol-gel technique [4]. In many cases the metallic phases lose their initial properties and uncontrolled reactions take place. To avoid these inconvenients, we have developed iron based composites on mesophase pitch (MP).

A series of composites, MP with carbon-coated nano iron (NC/Fe) and with iron oxide (Fe_2O_3 - Irox), ranging from micro scale to nano scale, have been studied [5, 6]. The magnetic properties depend on the iron dispersion method and the structural feature induced by the thermal treatment at 460°C. The MP-iron composites can be developed as materials with extremely large applications from memory materials to EMI shielding using a large spectrum in concentrations below and over percolation threshold. The aim of this paper is to present the structural and physical properties of the nano iron composites.

2. Experimental

The carbon matrix precursor (mesophase) was a petroleum pitch with softening point 70°C and high solubility to quinoline (99.55) and the carbon-coated nano iron (NC/Fe) was synthesized by laser pyrolysis in a mixture ethylene/$Fe(CO)_5$ according to the procedure described in [7]. Grain sizes, 6-10 nm, were evaluated by using HRTEM. These nanoparticles are iron coated with a carbon shell.

The iron oxide (Fe_2O_3) powder was obtained by a usual chemical process of alkaline reduction and it has Fisher diameter by 0.1 μm.

The composites were prepared in series of 0.05 - 1.5 wt % for carbon-coated nanoiron and 1 - 10 wt % for iron oxide [8]. The carbon-coated nano iron and iron oxide were mixed with petroleum pitch by stirring at 100°C for 30 minutes.

The composites were heat treated in argon atmosphere (1 atm), at a rate of 1°C/min, up to 460°C and were maintained at this temperature for 3 hours.

The optical properties were studied by using a Carl Zeiss NU 2 microscope and the structure by X-Ray Diffraction and Small Angle Neutron Scattering.

Thermal analysis was made by using a DTA model Q 1500D in argon atmosphere.

The DC resistivity was analyzed by a home made piston cylinder (PC) high pressure apparatus with Teflon die and HSS anvils. The samples were compressed at ~ 0.1 GPa. The electrical resistance was measured with a digital multimeter.

The dielectric properties were also studied by loss tangent using a Q-meter, model FERISOL, ranging from 0.2- 25 MHz.

The coercivity and the saturation magnetization were measured using a Vibrating Sample Magnetometer (VSM, 7300).

3. Results

The morphology induced by additives (carbon-coated nanoiron and iron oxide) and by the heat treatment of the composites is shown in Fig. 1. MP with 1 wt % Fe_2O_3 composite has coalescent mesophase spherules. The structure of MP is almost the same with the structure of MP with 1 wt % NC/Fe composite. At this temperature, the mesophase stage was surpassed and the structure is like a semicoke.

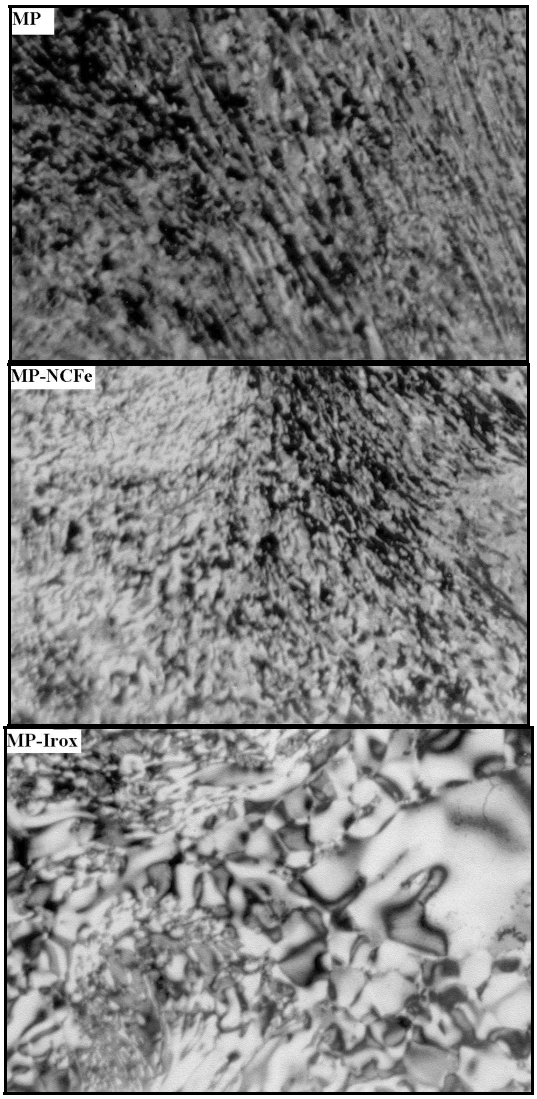

Fig. 1. Optical micrographs for MP, MP-NCFe and MP-Irox

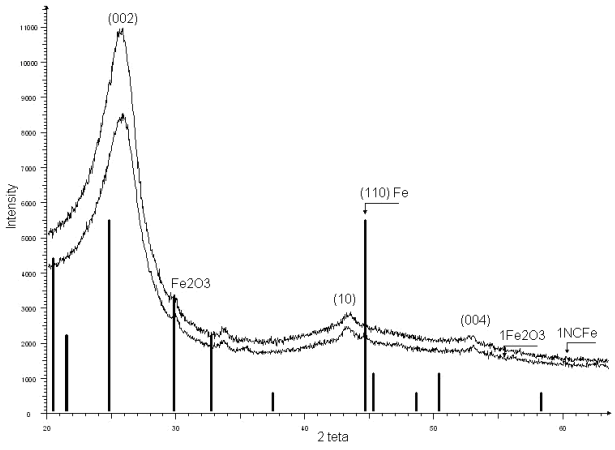

Fig. 2. XRD for MP with 1% NC/Fe and MP with 1% Iron oxide

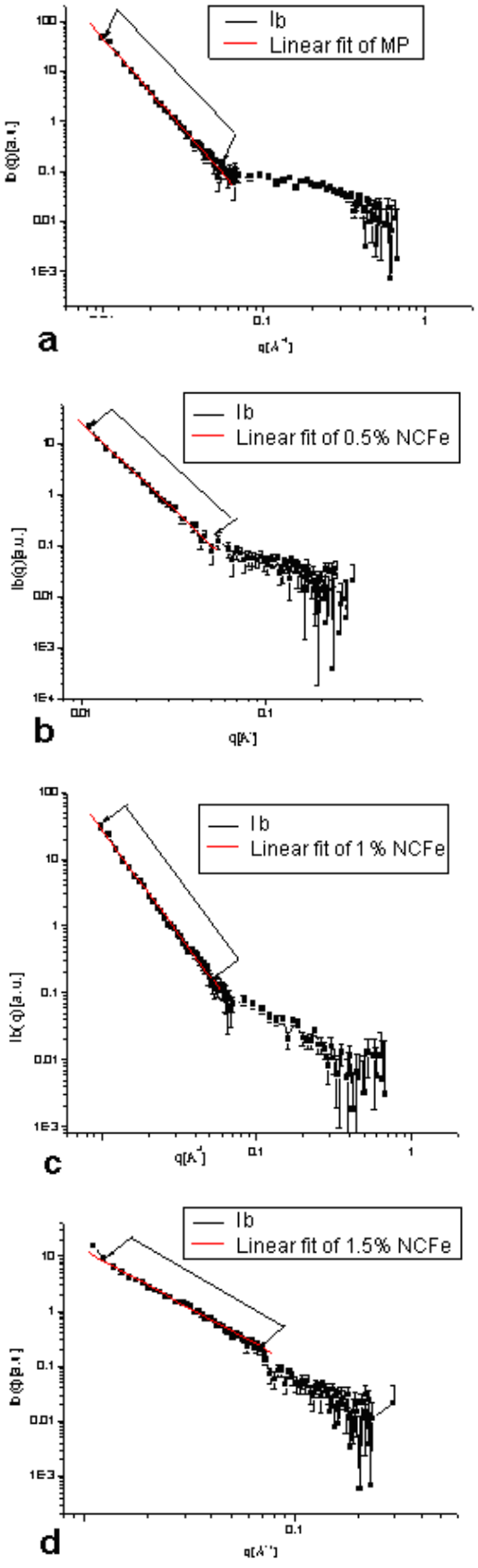

Fig. 3. SANS-scattering in the logarithmic coordinates for 0; 0.5;1;1.5% NC/Fe, after the subtraction of flat background

Table 1. The characteristic parameters of linear fitting of the experimental curves are presented. By S is denoted the slope of the experimental scattering curves and D_s is the surface fractal dimension.

MP-NCFe	S	D_s	q_{max} [Å^{-1}]
1.5 wt%	2.1 ± 0.03	2.1 ± 0.002	0.05
1 wt %	3.13 ± 0.04	2.87 ± 0.04	0.05
0.5 wt %	3.42 ± 0.06	2.58 ± 0.06	0.05
0 wt %	3.63 ± 0.04	2.37 ± 0.04	0.05

Thermo-differential analysis confirms the structural modification in composites (Table 2). V_{max} represent the maximum rate reaction and it is increased by the presence of Fe_2O_3 and decreased by NC/Fe. The composites with iron oxides have the same behavior as MP. The mass loss is not influenced by iron oxide microparticles. The NC/Fe composite presents a different behaviour. The volatiles are adsorbed by nanoparticles and for this reason the first peak is shadowed. The second peak is assigned to volatile desorption and the third peak is assigned to massive residual volatile desorption in MP.

Table 2. Thermo-gravimetric analysis on MP, MP-NCFe 1 wt % of and MP-Irox 1 wt %

Material	%Δm	T_I°C	T_{II}°C	T_{III}°C	%Δm_{330}° C	V_{max}
MP	41.5	140-200	362	402-418	20.5	0.256
1% Fe_2O_3	42.1	160	326-342	400	22.6	0.276
1% NC/Fe	37.8	-	345	360-390	18.3	0.209

The electrical resistivity of the composites (table 3) has distinctive features and gives us a rough idea of the dimension dependence when micro and nanoparticles are added. The two series of composites have an inflection at 0.5wt % NC/Fe and 7wt % Fe_2O_3, where the resistivity increases about two times. For the composite with 1.5wt % NC/Fe, the resistivity increased very much and for the composite with 10wt % Fe_2O_3, the resistivity decreased.

Table 3. Electrical resistivities for composites NC/Fe and Fe_2O_3

MP-NCFe (wt %)	Resistivity (ohm×m)	MP-irox Fe_2O_3 (wt %)	Resistivity (ohm*m)
0.05	36.3×10^3	1	8.21×10^3
0.1	31.5×10^3	3	5.78×10^3
0.5	50.3×10^3	5	6.52×10^3
1	43.8×10^3	7	14.6×10^3
1.5	137×10^3	10	2.12×10^3

Table 4. Dielectric losses (tgδ) and dielectric constant (k)

Frequency range, (kHz)	1 wt % Fe_2O_3 tgδ	1 wt % NC/Fe tgδ	1wt % Fe_2O_3 k, (F/m)	1 wt % NC/Fe k, (F/m)
200 - 2800	0.1583	0.0845	1.1542	1.1143
3200 - 5000	0.0739	0.0345	1.1429	1.3280
5500 - 8500	0.0528	0.0338	0.9396	0.9419
9000 -11500	0.0517	0.0533	0.9969	0.9933

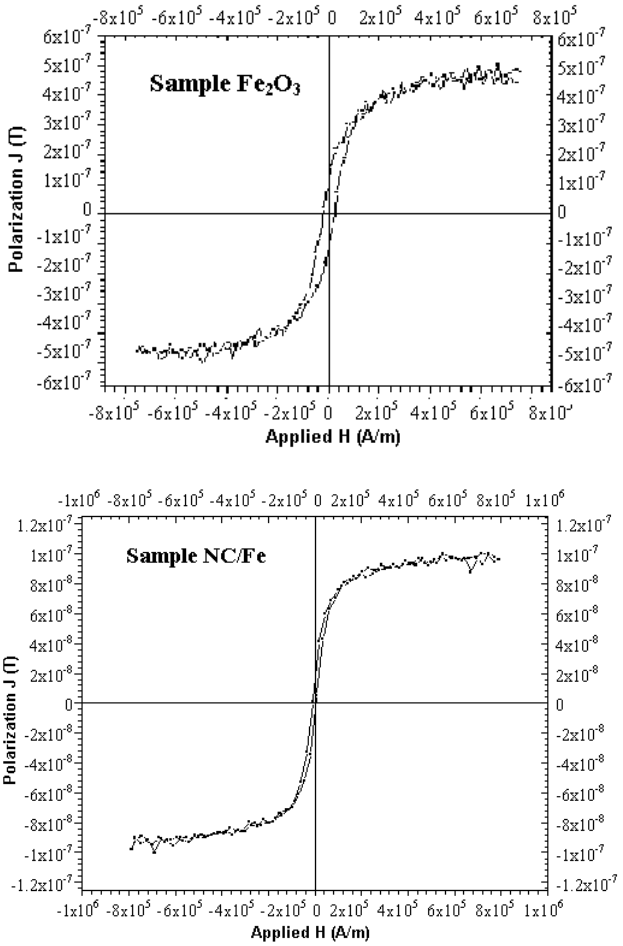

Fig. 4. Hysteresis loop for MP-Irox and MP-NCFe samples

4. Discussion

The structures of MP with nano iron composite (MP-NCFe) and MP with iron oxide composite (MP-Irox) are very different. MP with 1 wt % Fe_2O_3 composite has coalescent mesophase spherules. The structure of MP is almost the same with that of MP with 1 wt % NC/Fe composite. At this temperature, the mesophase stage was surpassed and the structure is like a semicoke.

The X-Ray Diffraction pattern of the powder (Fig. 2) shows a sharper (002) peak for MP-NCFe composite. For the MP-Irox composite, we can observe that the iron oxide is reduced in the presence of carbon to an excess of iron. Large but well defined (10) and (004) peaks of MP-NCFe are associated with the catalyst role of iron.

The SANS-scattering curve, I(q), the powders presents a complex shape. In the log-log representation (figure 3) can easily be observed two domains due to the different contributions. The lower q ranges between 0.01-0.05 $Å^{-1}$ (corresponded to the large objects, further we will named these clusters) exhibit the power law scattering behavior. We made a linear fit in log-log coordinates on this range of q values. The results are shown in the table 1 and indicated the presence of big clusters with fractal properties. The size of clusters ($d=2\pi/q$) are greater than 125 Å. The upper limits cannot be determined, because are beyond the instrumental limits of the detector. The slope increases with increase the amount of the additive. All the samples present surface fractal properties with one exception, namely 1.5 wt % NC/Fe. For the latter, the clusters present mass fractal properties (D_m represent the mass fractal dimension, $D_m=2.1\pm0.03$). The roughness of the surface fractal clusters and surface fractal dimension increase with decreasing the quantity of additive. From these we conclude that the additive content has an important role in the development of the structure at this length scale. The small additive content (0.5-1) wt % increases the roughness ($Ds_{1\%Nc/Fe}=2.87\pm0.04$; $Ds_{0.5\%NC/Fe}=2.58\pm0.06$) and induces a condensation in the skeleton of the clusters. The relative high additive content shows an anti-agglutinant effect, and determines the formation of mass fractal clusters. The quantity of additive has a key role in the development of the structure at this length scale. The smaller additive content (0.5-1) wt % increases the roughness of the surface fractal clusters and induces a condensation in the skeleton of the clusters, since the greater additive content produces an anti-agglutinant effect and determines the formation of mass fractal clusters [9, 10].

The composites with iron oxide have the same behavior as MP. The mass loss is not influenced by iron oxide microparticles. Thermal decompositions have three temperature stages and the total loss is around 41-42 wt % (Table 2).

The NC/Fe composite has another behavior. Because the volatiles are adsorbed by nanoparticles the first peak is shadowed. The second peak is assigned to volatile desorption with a slow conversion to carbon. The third peak is assigned to massive residual volatile desorption that appears at regular pyrolysis in MP. The catalytic effect of the iron nanoparticles being slower than desorption phenomena does not have a significant contribution to carbon conversion. The kinetic (V_{max}) is largely decreased when nanoparticles are present in initial raw materials.

By comparison, the two series of composites have an inflection at 0.5 wt % NC/Fe and 7 wt % Fe_2O_3, where the resistivity increases about two times (table 3). For the composite with 1.5 wt % NC/Fe, the resistivity increased very much and for the composite with 10 wt % Fe_2O_3, the resistivity decreased.

The dielectric losses are more frequency sensitive than the dielectric constant. At low frequency the dielectric losses are more significant in samples where Fe_2O_3 is added. At higher frequency the effects are similar for both materials added in MP (table 4). The dielectric constant has a maximum for the sample with 1 wt % NC/Fe at a frequency range of 3200-5000 kHz.

The magnetic properties, especially the hysteresis, are different in the two samples (figure 4). The MP with NC/Fe has a narrower hysteresis loop than MP with iron oxide.

This behavior appears can be correlated with the particle sizes. The iron oxide particles have dimensions about micrometers and the carbon-coated iron particles have dimensions about nanometers. Thus, at room temperature some iron coated particles can be superparamagneic.

5. Conclusions

The insertion of micro and nanoparticles in petroleum pitch, along with thermal treatment in the range where MP is developed, induce morphological and structural transformations. The addition of iron based particles influences the electric and magnetic properties, depending on size, type of particles and thermal treatment. The result is a material with a large area of application in electric and electromagnetic devices.

Acknowledgments

Project NATO-SfP 974214, Carbon ceramic materials, 2000-2004.

References

[1] S. Miyanaga H. Yasuda, A. Hiwara Macromol Sci-Chem **A27**, 1347 (1990).
[2] S. Huaihe, C. Xiaohong et all, Carbon **41**, 3037 (2003).
[3] Jun-ichi Ozacki, Yoko Yoshimoto, et all, Proceeding of International Conference CARBON'02, Beijing, China, (2002).
[4] Weize Wu, Zhenping Zhu, Zhenyu Liu, Carbon **40**, 787 (2002).
[5] E. P.Sajitha, V. Prasad, S.V.Subramanyama, S. Eto, Kazuyuki Takai, T. Enoki, Carbon **42**(14), 1127 (2004).
[6] U. Narkiewicz, N. Guskos, W. Arabczyk, J. Typek, T. Bodziony, W. Konicki, G. Gazsiorek, I. Kucharewicz, E.A. Anagnostakis, Carbon **42** (14), 2815 (2004).
[7] F. Dumitrache, I. Morjan, et all, Proceeding of International Conference CARBON'03, Oviedo, Spain, (2003).
[8] G. A. Rimbu, C. Banciu, A.M. Bondar, I. Pasuk, I. Stamatin, I. Morjan, I. Sandu, Proceeding of International Conference CARBON'03, Oviedo, Spain, (2003).
[9] I. Ion, A.M. Bondar, Yu. Kovalev, C. Banciu, I. Pasuk, J. Optoelectron. Adv. Mater. **8**(2), 624 (2006).
[10] I. Ion, C. Banciu, F. Barca, A-M Bondar, Y. Kovalev, A. Kuklin, I. Pasuk, Poverhnost, Rentgenoskie, Sinhrotronnyie I Neitronnye Issledovaniya **6**, 84 (2006).

*Corresponding author: cbanciu@icpe-ca.ro